Regenerative Engineering and Translational Medicine
https://doi.org/10.1007/s40883-025-00445-6

ORIGINAL RESEARCH

3D Printing of Enzymatically Softening Hydrogel Biomaterials

Olivia P. Dotson[1,2] · Sherina Malkani[2,3,4] · Inkyung Kang[2,3] · Cole A. DeForest[1,2,3,5,6,7] · Kelly R. Stevens[1,2,3,8,9]

Received: 6 February 2025 / Revised: 23 May 2025 / Accepted: 31 May 2025

Abstract

Purpose 3D printing has accelerated tissue engineering by enabling rapid fabrication of bioprinted tissues from a variety of soft biomaterials. Yet, an ongoing challenge is that for many bioprinting technologies, the materials (bioinks) need to be printed "stiff" (i.e., G′ > ~ 15 kPa) so that the fabricated tissue constructs retain high resolution and shape fidelity. Conversely, softer materials tend to generally be more supportive of cellular phenotype and function. To bridge this gap, we sought to develop a hydrogel system that would expand bioprinting access to softer materials, while retaining the resolution of fabricated spatial features.

Methods We developed a photopolymerizable copolymer hydrogel system consisting of nondegradable synthetic and proteolytically degradable natural polymers. Varying the overall polymer content, as well as the ratio between the poly(ethylene glycol) and gelatin species, we generated a library of lithographically printable hydrogel formulations with differing initial stiffnesses that could be further variably softened following enzymatic treatment using collagenase.

Results Varying the copolymer composition and overall concentration resulted in the creation of gels whose initial stiffness ranged from 82 to 2 kPa and could be subsequently softened up to 20-fold upon enzymatic treatment. When 3D-printed via digital light processing (DLP), softened gels maintained higher structural integrity than those with matched initial stiffness. Softened gels supported greater endothelial cell perfusion-based seeding compared to those untreated while maintaining high cell viability.

Conclusion Our material system presents a simple solution to the ongoing challenge of 3D-printing soft materials with high resolution.

Future Work In future studies, we will develop post-print softening materials with bio-invisible stimuli to expand applications to in vivo softening of biomaterial tissue mimics.

Lay Summary 3D-printing has become popular in tissue engineering applications, but printing complex, organ-like structures with soft materials remains challenging. We created a material that can hold patterned shapes and small printed structures using a post-print softening technique with a degrading enzyme. We found that different formulations of this hydrogel material offer varying stiffness levels (G′ = 2 kPa–82 kPa) and can soften up to 20-fold with enzymatic treatment. Notably, this material retains the structure of 3D-printed open channels even after significant softening, and cells respond well when seeded in these channels. This demonstrates the promise of post-print softening to create soft 3D-printed materials.

Keywords Biomaterials · 3D-printing · Hydrogel · Tissue engineering

Introduction

The field of tissue engineering has made major strides in fabricating bioprinted tissues that mimic the intricate architectures of vascularized soft organs [1–4]. Within this field, digital light processing (DLP) holds promise for fabricating spatially patterned structures in bioprinted tissues of scaled sizes because fabrication can be parallelized to simultaneously and independently print millions of voxels per time step [5–7]. DLP-based additive manufacturing thus enables relatively quick printing (< 30 min) by flashing 2D-light patterns layer-by-layer into a photopolymerizable pre-polymer resin, as opposed to the more tedious voxel-by-voxel patterning for many other approaches [6, 8]. This method affords control over features in the x–y plane, and adding a photoabsorber (e.g., tartrazine) can also enable precise feature patterning in z. For example, Grigoryan and colleagues used DLP with

Extended author information available on the last page of the article

acrylated synthetic materials to 3D-print a series of hydrogel structures containing Hilbert curves, a torus knot, and an intricate alveolar model using a 50-µm pixel projector [9].

Yet, deploying DLP to fabricate complex features within biomaterials with mechanical properties that mimic those of soft organs (< 10 kPa) has remained challenging because such "soft" materials do not typically retain high shape fidelity upon printing [10, 11]. As a result, DLP studies that have achieved complex architectures in soft materials have been primarily limited to producing relatively simple, near planar constructs, with features patterned only in the x–y plane [12]. For structures printed using DLP in three dimensions, the modulus of the printed tissues has typically been substantively higher than that of the physiological stiffness of the target organs. For example, the structures produced by Grigoryan et al. had storage moduli (G′) from 10–50 kPa compared to that of 2–10 kPa for the target organs, up to a 25-fold difference [9, 13, 14].

To address this challenge, some groups have recently sought to achieve high resolution in soft prints by dynamically tuning hydrogel stiffness post printing. As one example, Wang et al. used photopolymerization of gelatin methacryloyl/methacrylate (GelMA) and hyaluronic acid methacrylate (HAMA) as a crosslinked network to 3D print stiff hydrogel constructs with complex structure or vascular architecture. Enzymatic digestion of the HAMA with hyaluronidase was then deployed to create a softer gel that generally retained the structural integrity of the originally printed construct [15].

Here, we translate this concept of enzyme-mediated 3D-print softening into a different hydrogel system newly incorporating a synthetic polymer component. We sought to print copolymer constructs with poly(ethylene glycol) diacrylate (PEGDA) and GelMA, whereby GelMA can be selectively and enzymatically degraded post-printing with collagenase. To do this, we identified GelMA:PEGDA compositions with storage moduli ranging from 2 to 82 kPa, which were capable of 0–20-fold enzymatic softening. We then validated the retention of the 2D photomask and 3D DLP-printed features following enzymatic treatment. Finally, we demonstrated that this "print-then-soften" workflow enables printed features that support greater cell retention compared to constructs without softening.

Methods

Fabrication of the PEGDA/GelMA Hydrogel Network

Poly(ethylene glycol) diacrylate (PEGDA) powder (6000 Da, Allevi, Inc by 3D Systems) was reconstituted in phosphate buffered saline (PBS) at 50%w/v. Gelatin methacrylate (GelMA, 300 bloom, degree of substitution 53%, Allevi, Inc by 3D Systems) lyophilized beads were reconstituted in PBS at 40% w/v. Both pre-polymer solutions were set on a heat block to warm at 37 °C and then added to a microcentrifuge tube in the desired ratio along with PBS and photoinitiator lithium phenyl-2,4,6-trimethylbenzoylphosphinate (17 mM LAP, Sigma-Aldrich) and quickly vortexed and centrifuged (Table S1). This solution was then pipetted onto a hydrophobic Rain-X- treated glass slide and then casted between another glass slide with a 0.3-mm silicon spacer. Then, this was placed under an S1500 OmniCure (Excelitas Technologies) for 30 sec to2 min under 365 nm light at a 5 mW/cm^2 light intensity.

To evaluate feature retention, the "W" hydrogels were cast similarly, yet between coverslips for greater light penetration with the outline of the "W" as a photomask. A radical scavenger (5 mM TEMPO) was also incorporated in the formulation to prevent any off-target curing.

Rheological Characterization of PEGDA/GelMA Hydrogel

Performed rheological measurements (Anton Paar MCR-301) on 20-µL casted hydrogels with a 5-min time sweep using an 8-mm-diameter parallel plate at room temperature (25 °C). Strain = 1.0, angular frequency = 10 rad/s, amplitude gamma = 1%, angular frequency omega = 6.2831853 1/s.

Enzymatic Degradation of Hydrogel Materials

Collagenase Type I from *Clostridium histolyticum* (Sigma-Aldrich) was suspended in 1X Hanks Buffered Salt Solution (HBSS) along with 3 mM (0.003 M) $CaCl_2$ to make a 0.5 or 1.0 mg/mL collagenase treatment solution. The casted hydrogels were treated with 0.5 mg/mL collagenase for 14 h. Hydrogels were placed in a 48-well plate and fully submerged in the (~ 500 µL) collagenase solution and left overnight to shake in an incubator at 37 °C. The 3D-printed hydrogel constructs were treated with 1.0 mg/mL collagenase for 24 h. Hydrogel constructs were placed in a 12-well plate and fully submerged in the (~ 1.0 mL) collagenase solution and left to shake in an incubator at 37 °C. Following this treatment, hydrogels were washed twice with PBS prior to evaluation. Note that this protocol from previous literature was adapted to account for the varied size and geometry of the hydrogel construct [16].

DLP Printing

A digital light processing (DLP) printer was used to cure the pre-polymer formulation layer-by-layer onto a build platform. To do this, the pre-polymer precursor was first injected onto a polydimethylsiloxane (PDMS)-coated petri dish warmed to 40 °C to ensure the solution remained in its liquid state during the print. The porosity of the PDMS coating functioned as an oxygen inhibition layer between the petri dish and the cured bioink to reduce sticking of the printed object [17]. Then, the build platform was lowered into the solution hovering 50 µm

above the PDMS plate as the first layer was cured with a flash of light from the projector. The build platform then lifted 50 µm and another light projection cured the next layer and continued until the final layer was projected. The light intensity at 405 nm from the projector was set using an intensity meter (308 Meter Optical Associates Inc., San Jose, CA) at 24.5 mW/cm^2 for each print.

Defining Percent Feature Retention

"W" logo features were quantitatively analyzed using an overlay of the original CAD photomask with hydrogel images to measure excess area or void space in the casted gels. The percent feature retention was then determined by the following equation:

$$[1 - (\text{Excess Area outside shape} + \text{Void Area inside shape}) / \text{Area of Desired Shape}] \times 100 \quad (1)$$

80% was designated a feature fidelity threshold of "High" labeled with a light grey square and this included the formulations: 15wt% polymer | 0%GelMA, 15wt% polymer | 25%GelMA, 15wt% polymer| 50%GelMA, 10wt% polymer | 25%GelMA, 10wt% polymer | 0%GelMA, 5wt% polymer | 0%GelMA, and 5wt% polymer | 25%GelMA. Between 80% and 20% was "Moderate" labeled with a grey square and this included the formulations: 5wt% polymer | 50%GelMA and 10wt% polymer | 50%GelMA (enzyme-treated) formulations. 20% and lower was designated with "Low" indicated by a dark grey square and consisted of the 5wt% polymer | 25% and 50%GelMA (enzyme-treated) formulations.

Cell Seeding in Printed Constructs

The 15wt% total polymer | 25% GelMA (11.25:3.75wt%| PEGDA:GelMA) hydrogel structure with perfusable channels was printed in a sterile biosafety cabinet. The channels were coated with fibronectin 5 µg/cm^2 for 30 min and then washed briefly with 1X HBSS. Human umbilical vein endothelial cells (HUVECs) were seeded by filling the reservoirs with 5 M HUVECs/mL and incubating on a rocker at 37 °C to enable flow into the channels. These gels were flipped upside down after 2 h to ensure even coverage of the channel surface. After another 2 h, the gels were then flipped again and incubated for 3 days for this study. Cell viability was assessed via staining with Ethidium Homodimer-1 and Calcein AM followed by confocal imaging (Nikon Elements AR Confocal). Viability was quantified in ImageJ and CellProfiler as Number of Live cells/(Sum of Live and Dead cells) [18]. Further statistical testing of the data was performed using GraphPad Prism.

Results

Light-Sensitive Materials with Tunable Storage Moduli for Bioprinting

We set out to develop a tunable softening material system for bioprinting. To do this, we created a copolymer hydrogel network consisting of both synthetic (PEGDA) and natural (GelMA) components (Fig. 1). As both components are polymerized via a radical-mediated chain growth mechanism, both the total polymer content and the relative ratio between the PEGDA/GelMA can be readily changed during formulation to tune the mechanical properties of the final hydrogel. We hypothesized that GelMA could be selectively degraded from this copolymer network via collagenase treatment while leaving the PEGDA intact, thereby facilitating post-print softening of the hydrogel while retaining its structure.

To test this hypothesis, we first set out to establish the initial storage moduli that could be achieved prior to enzymatic treatment by altering both the total polymer content and the ratio of GelMA to PEGDA (prior to any enzymatic treatment). To do this, we screened GelMA/PEGDA formulations containing 0, 25, 50, 75, or 100% GelMA content, and total polymer concentrations of 5, 10, or 15wt% (Fig. 2; light colored bars). We found that the storage moduli for these hydrogel formulations range from 30 to 80 kPa for 15wt% total polymer content, 9 to 32 kPa for 10wt% total polymer content, and 2 to 8 kPa for 5wt% total polymer content, as measured via in situ rheometry.

To assess if these hydrogels could be softened upon enzymatic degradation, we then treated each hydrogel with collagenase (0.5 mg/mL for 14 h) and then quantified the storage moduli. For the hydrogels with 15wt% total polymer content, those with 25% GelMA softened from 65 to 40 kPa (1.6-fold softening), those with 50% GelMA softened from 57 to 14 kPa (4-fold softening) and those with 75% and 100% GelMA completely degraded after enzymatic treatment (Fig. 2A; dark colored bars). We observed a similar trend for the hydrogels with 10wt% total polymer content, those with 25% GelMA softened from 27 to 12 kPa (2.3-fold softening), those with 50% GelMA softened from 15 to 0.9 kPa (17-fold softening), and those with 75% and 100% GelMA completely degraded (Fig. 2B). For hydrogels with 5wt% total polymer content, those with 25% GelMA softened from 4 to 0.2 kPa (20-fold softening), and those with either 50, 75, or 100% GelMA fully degraded. No stiffness changes were observed for gels with 0% GelMA (100% PEGDA), regardless of total polymer content, confirming that PEGDA is not degradable via collagenase (Fig. 2).

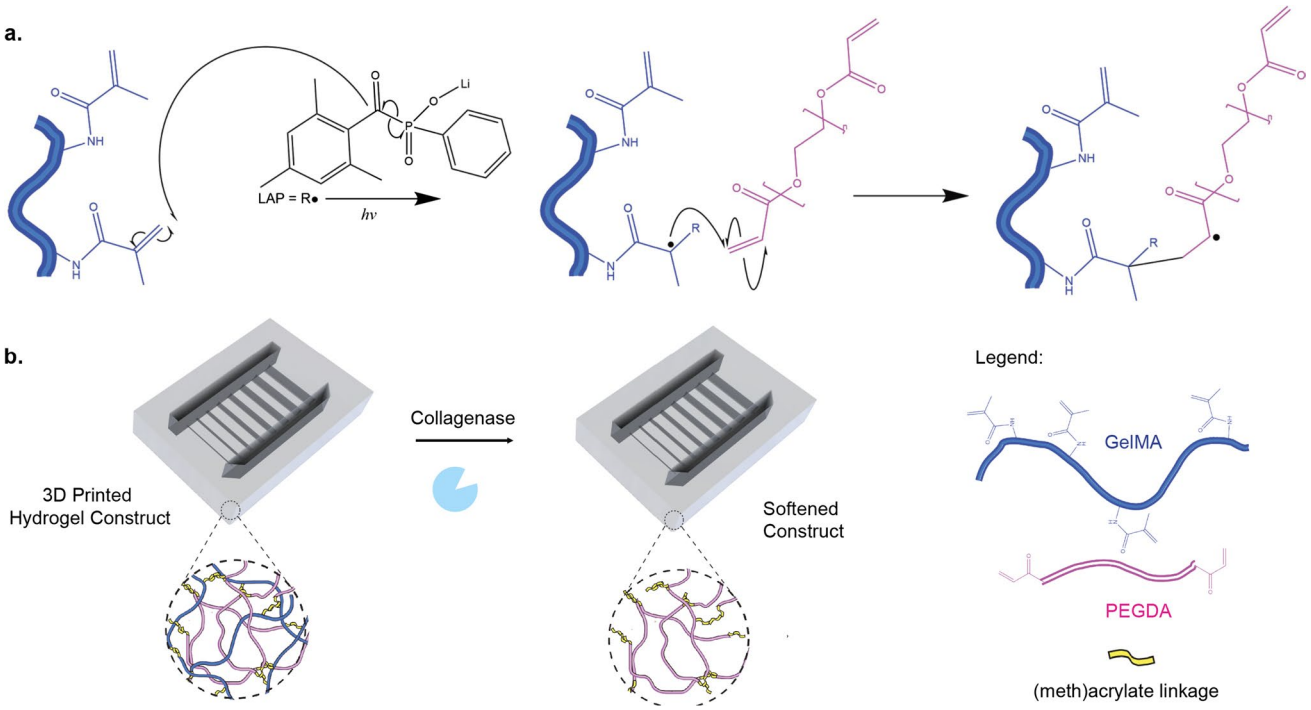

Fig. 1 Mechanism of hydrogel crosslinking and enzymatic softening. **a** PEGDA and GelMA are cured into a dual network hydrogel via radical-mediated chain-growth polymerization. Here, LAP is used as a photoinitator and responds to 365 and 405 nm light. **b** Collagenase treatment of the printed polymer networks yields bulk construct softening via selective GelMA degradation

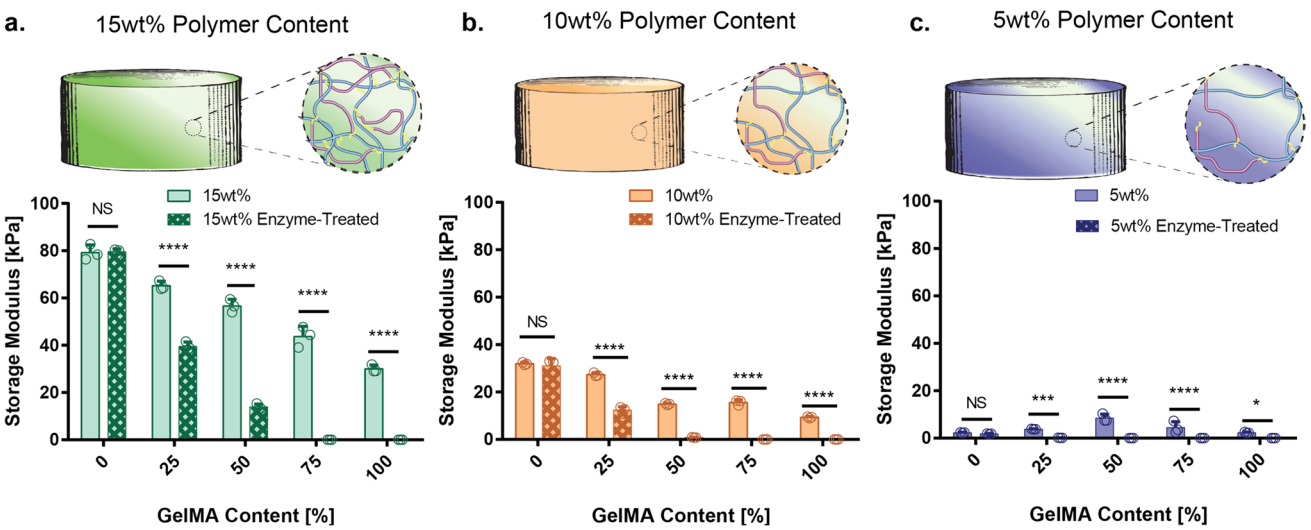

Fig. 2 Tunable enzymatic softening of hydrogel formulations. **a** Rheological measurements of the hydrogel stiffness before and after enzymatic treatment with 15wt% total polymer content, **b** 10wt% total polymer content, and **c** 5wt% total polymer content. Error bars indicate SD. $^{****}P < 0.0001$, $^{***}P < 0.001$, $^{**}P < 0.01$, $^{*}P < 0.05$ by two-way ANOVA, Sidak Correction

Photopatterned Spatial Feature Retention in Varying Hydrogel Formulations After Softening

Encouraged by the tunable softening and expansive range of moduli observed in these results (80 to 0.2 kPa), we next examined the extent to which photomask-patterned features would be retained in varying GelMA/PEGDA formulations both before and after softening. We photopolymerized hydrogels in the shape of the University of Washington's "W" logo by exposing the prepolymer solution to 405 nm

light through a photomask (Fig. 3). We assessed formulations from the 5, 10, and 15 total polymer wt% conditions, varying between 0 and 100% GelMA content (Fig. 3A). The photomask was designed to have one down stroke of the "W" to be 1.2 mm wide and the opposite up stroke to be 0.6 mm wide (Fig. 3B). The hydrogels were swelled to equilibrium in phosphate buffered saline (PBS) and treated with collagenase overnight.

We found that 75–100% GelMA hydrogels fully degraded after softening; these hydrogels were excluded from the full feature fidelity comparison after softening. For all other formulations, we quantified the percentage of the photomask area that was occupied by hydrogel after patterning and then assigned thresholds for feature fidelity (Eq. 1). All non-treated formulations initially had over 73% fidelity of features from a 2D photomask. Only the hydrogel with the lowest total polymer content (5wt%) and highest GelMA content (50%) had < 85% feature retention prior to enzymatic treatment.

The feature retention post-enzymatic treatment was then quantified and compared to the non-treated conditions. We found that despite the softening observed in these hydrogel formulations (Fig. 2), the fabricated "W" hydrogels largely maintained their geometry and overall size for most formulations. Specifically, all but two hydrogel formulations had > 71% feature fidelity retention relative to the initial mask design. Notably, most of the feature fidelity retention scores showed no significant change post-enzymatic treatment, highlighting that enzymatic softening did not negatively impact construct geometry (Fig. 3B, C). For example, the 15wt% total polymer| 50% GelMA exhibited retained all of its features despite its fourfold softening (Fig. 3A, C;

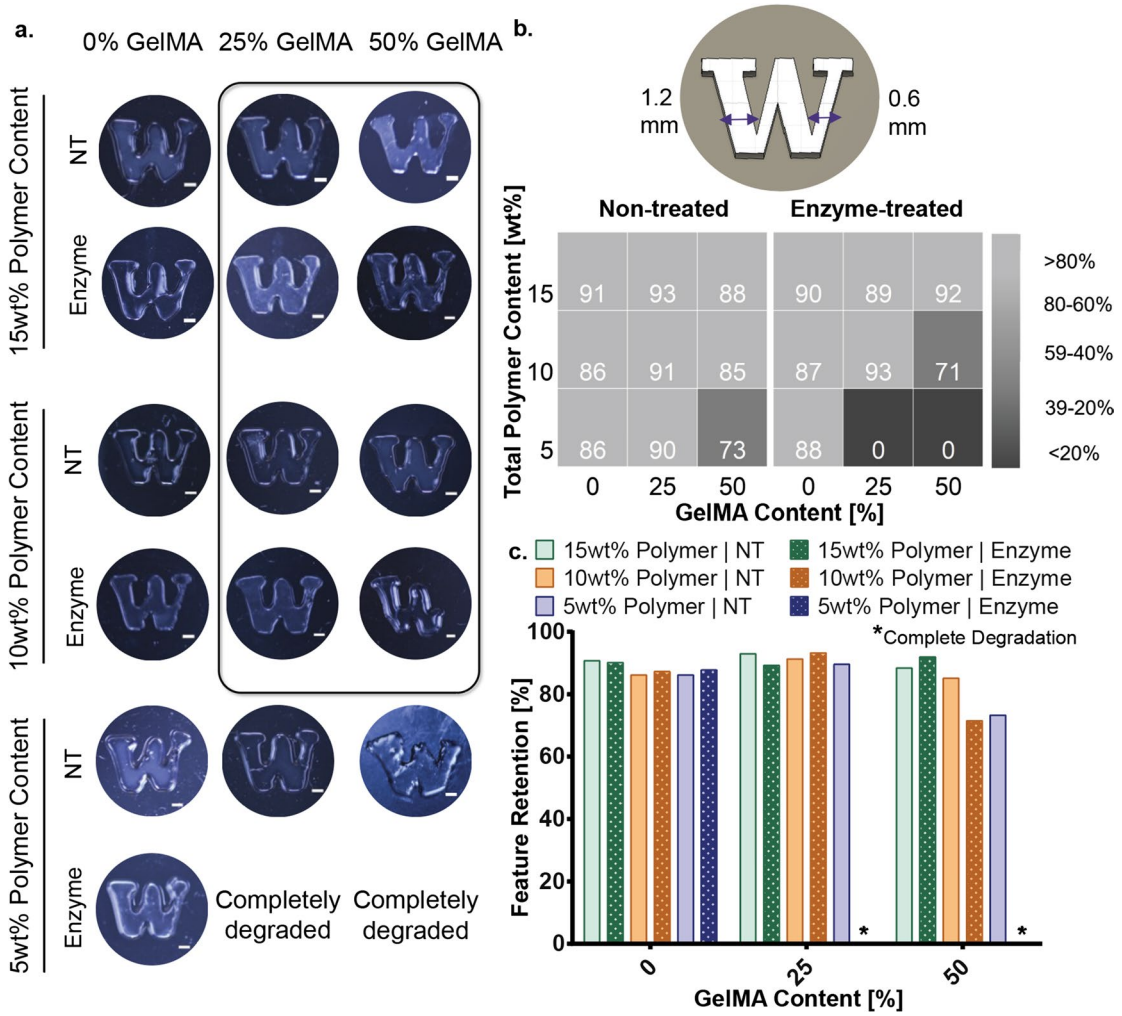

Fig. 3 Feature retention of photopatterned and softened hydrogels. **a** Hydrogels photopolymerized into "W" shapes for assessment of feature retention before and after enzymatic softening; scale bar, 1 mm. **b** CAD model of the University of Washington "W" logo photomask and feature retention score from overlay of model for each casted "W" hydrogel. **c** Comparison of percent feature retention scores for "W" hydrogels before and after enzymatic treatment

Fig. 2A). Some patterning fidelity was lost with 10wt% total polymer content hydrogels once GelMA content reached 50%. After softening, this condition lost the smaller 0.6-mm patterned feature but retained the larger 1.2-mm feature (Fig. 3A, C). We did note that this method failed for hydrogels with 5wt% total polymer content, as these samples completely degraded after enzymatic treatment (Fig. 3A–C).

3D-Printed Constructs Retain Spatial Features After Softening

Encouraged by these 2D photopatterning results, we next sought to assess the extent to which features would be retained after 3D-printing and enzymatic softening. For these studies, we used DLP printing, in which a prepolymer solution or "bioink" is cured with light projection of a slice of the construct design layer-by-layer onto a build platform (Fig. 4). For these studies, we designed a construct with a "ladder" of hollow channels with decreasing diameters from 800 to 100 µm, flanked by two side reservoirs that provide filling (inflow) and flow through (outflow) paths for the channels (Fig. 4B, C). This design enabled us to assess resolution of the printed constructs by characterizing the extent to which each printed channel can later be filled with an indicator dye, with the smallest open channel filled with dye indicating approximate print resolution for each hydrogel formulation (Fig. 4D).

We chose to use the 15wt% total polymer content formulations for printing studies as these formulations received the highest feature fidelity scores in photomask studies (Fig. 3). This particular formulation's high feature fidelity score (93%) is a measure of how accurate the photopatterned features are in the prescribed shape of the hydrogel. Thus, the 15wt% total polymer hydrogel with 25% GelMA was determined to be the material best fit to hold more complex 3D features when transitioning to applications in 3D-printing. Having been previously shown to respectively improve viscosity and prevent off-target light penetration glycerol and tartrazine were included in the hydrogel precursors for DLP printing studies [5, 9]. The 15wt% total polymer content formulations were thus printed with 0%, 25%, and 50% GelMA content using the ladder architecture. We found that the smallest diameter of open channels after swelling—but prior to enzymatic softening—was 500 µm for the 0% and 25% GelMA formulation and 600 µm for the 50% GelMA formulation. The printed constructs were then subjected to collagenase treatment. Interestingly, all three formulations retained their original

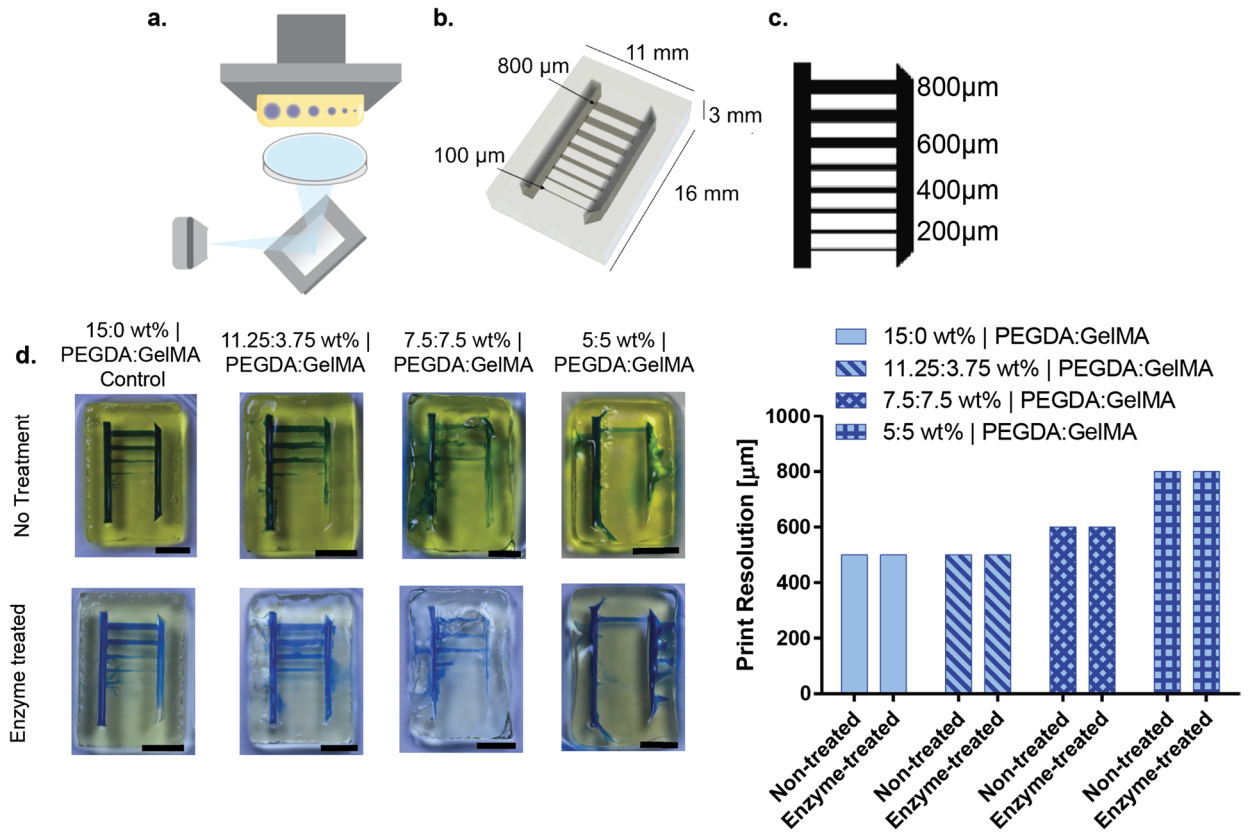

Fig. 4 Feature retention within softened 3D-printed constructs. **a** Schematic of DLP printing. **b** CAD model of ladder structure in bioprinted construct. **c** Photomask of the channel ladder construct with channel diameters ranging from 800 to 100 µm. **d** Enzymatic softening with resolution retention from non-treated (top) to 24 h enzyme treated (bottom); scale bar, 5 mm

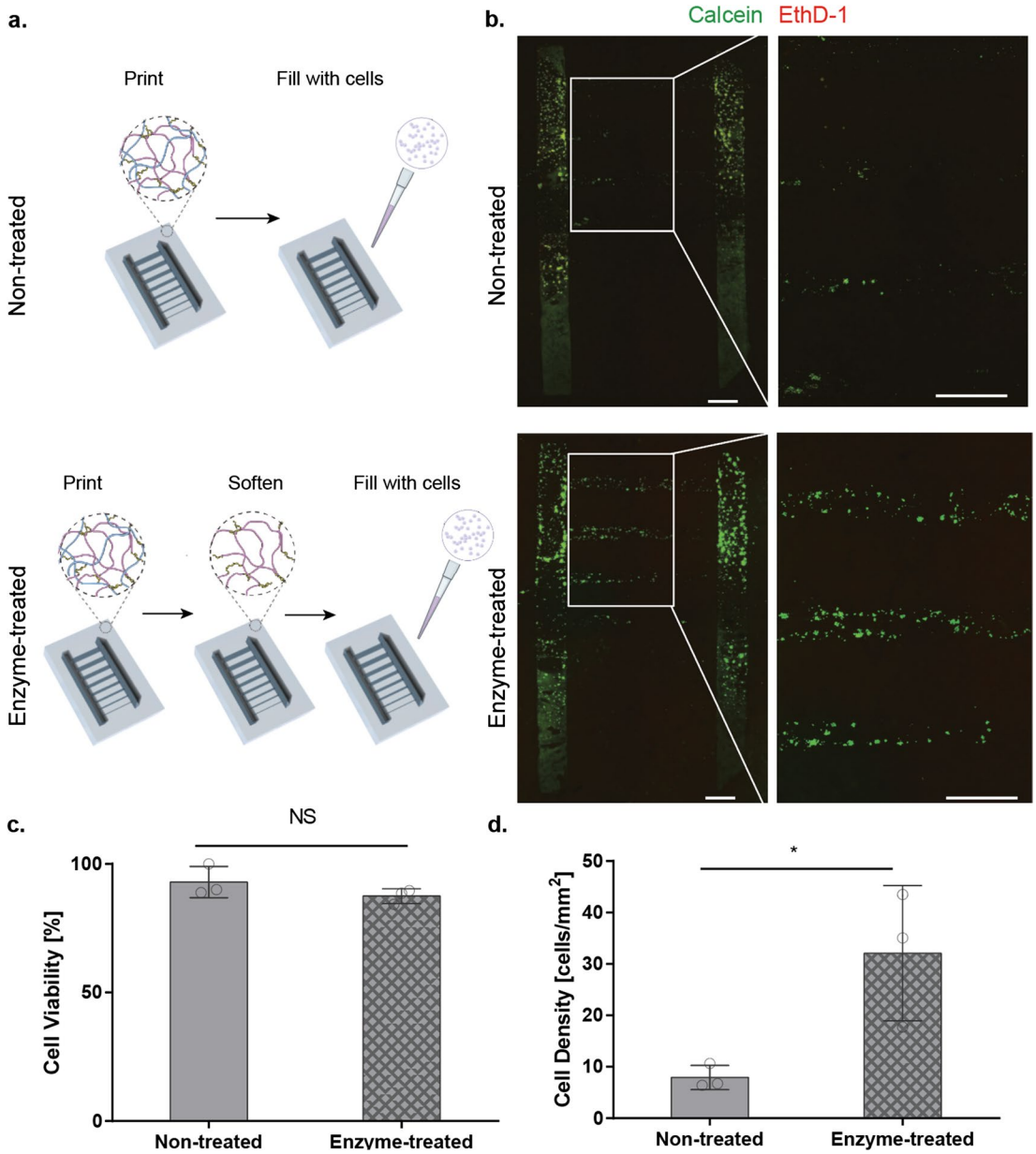

Fig. 5 Endothelial cell seeding in channels of softened constructs. **a** Schematic of workflow for fabrication, enzymatic softening, and cellularization of bioprinted constructs. **b** Maximum intensity projection of HUVECs seeded in channels of non-treated and enzyme-treated constructs at low magnification with higher-magnification inset images; Calcein AM Staining (green) and Ethidium Homodimer-1 (red); scale bars, 1 mm. **c** Quantification of viability of endothelial cells in the channels [$n = 3$, error bars indicate SD, $^*P < 0.05$ by one-tailed parametric t-test]. **d** Quantification of cell density of endothelial cells in the channels [$n = 3$, error bars indicate SD, $^*P < 0.05$ by one-tailed parametric t-test]

resolution via open channels. In summary, we observed that the collagenase-mediated gel softening did not significantly affect the geometry and resolution of the initial print.

Enzymatic Softening Supports Cellularization of Printed Channels

Finally, we investigated whether enzymatic softening would affect the extent to which endothelial cells could be seeded and adhered to the inside of the printed channels. We produced two printed hydrogels with the same initial total polymer content (15wt%) containing 25% GelMA. We then enzymatically softened one of these conditions but left the other untreated. Before seeding cells, the channels of both gels were coated with fibronectin for improved cell adhesion. Finally, we seeded human umbilical vein endothelial cells (HUVECs, 5 M/mL) into both the non-treated and enzymatically softened printed constructs. Interestingly, after

3 days, we found that enzyme-treated gels contained higher cell densities within the printed channels compared to their non-treated counterparts, perhaps either by retaining more cells or facilitating their adhesion to the sides of the channels (Fig. 5). Given that both gels were coated in fibronectin before cell seeding, this result indicates that post-print matrix softening can be a route to improve cell coverage in printed vascular constructs. This may be further explained as a result of the cells settling into the softened material matrix having a larger mesh size left after digestion of the GelMA (Fig. S1, S2).

Discussion

We have established a selectively degradable copolymer hydrogel system and have shown that this method can be used to soften 3D-printed tissue constructs. Validating this approach, our copolymer system consisted of a photocrosslinked network of both natural GelMA and synthetic PEGDA components. Treating the hydrogel with a collagenase selectively degrades the gelatin portion of the network leaving the acrylate crosslinks and PEGDA components intact, softening the gel by several fold.

As cells respond to dynamic mechanical cues presented in their local microenvironment, the stiffness of the surrounding cell environment has been shown to play a significant role in cell function, phenotype, and fate [19–21]. Thus, creating soft gel matrices allows us to more accurately model healthy organ tissue. Here, we found altering both the ratio of GelMA to PEGDA and the total weight percent of acryloyl crosslinks allows us to access a range of storage moduli from 2 to 82 kPa before softening, then further degrade to a storage modulus of 0.2 kPa after softening.

This hydrogel material system highlights GelMA and PEGDA for post-print softening of hydrogels to achieve and retain a higher resolution than directly printing low weight percent, soft hydrogel structures. Additionally, this post-print softening system could be translatable to other acrylate functionalizable, photopolymerizable natural polymers (e.g., methacrylated hyaluronidase and methacrylated alginate) with a degrading enzyme. This system would also work with other methods of additive manufacturing including extrusion-based printing, since the use of post-enzymatic treatment does not interfere with the initial print formation of the hydrogel structure.

Though these initial efforts do highlight the potential utility of a "print-then-soften" workflow, its current implementation is not without limitations, particularly as the collagenase trigger would likely impact phenotype and function of cells present during softening [22]. An alternative strategy could make use of more biologically inert softening treatments, such as those based on sortase chemistry, or bioorthogonal cleavage-type reactions to aid in high-resolution printing and softening of cell-laden materials [21, 23, 24]. Additional considerations for future studies will include screening alternative hydrogel formulations and properties, such as higher molecular weight polymers for the PEGDA or GelMA components to precisely tune initial stiffness. Another intriguing direction for our material system would be the incorporation of a methacrylated polyethylene glycol (PEGMA) as an alternative to PEGDA. Since the methacrylate chemistry is slightly less reactive than the acrylate, this would allow for an investigation of whether changes in functionalization would affect integration of the PEGMA and GelMA components into the hydrogel network.

Conclusion

This new approach to create bioprinted hydrogel materials with tunable mechanical properties enables the production of high resolution and cytocompatible engineered tissue constructs. This work could thus accelerate future basic and translational biomedical research applications, such as therapeutic tissues and human organ model systems.

Supplementary Information The online version contains supplementary material available at https://doi.org/10.1007/s40883-025-00445-6.

Author Contributions All authors contributed to the study conception and design. Material preparation, data collection, and analysis were performed by Olivia P. Dotson. The first draft of the manuscript was written by Olivia P. Dotson with all other authors providing substantial feedback prior to submission of the manuscript. All authors read and approved the final manuscript.

Funding This work was supported by the NIH R01DK128551 (K.R.S.), Wellcome Leap as part of the HOPE program (K.R.S.), W.M. Keck Foundation (K.R.S.), Allen Distinguished Investigator Award (K.R.S.), a Paul G. Allen Frontiers Group advised grant of the Paul G. Allen Family Foundation (K.R.S.), NIH Maximizing Investigators' Research Award (R35GM138036, C.A.D.), NIH Research Award (R21CA283686, C.A.D.), NSF Graduate Research Fellowship (2023353131, O.P.D.).

Data Availability All source data generated in these studies is available upon reasonable request to the corresponding authors.

Declarations

Ethics Approval This is an observational study. The University of Washington Research Ethics Committee has confirmed that no ethical approval is required.

Informed Consent Statement On behalf of all authors (Olivia P. Dotson, Sherina Malkani, and Inkyung Kang), the corresponding authors (Cole A. DeForest and Kelly R. Stevens) state that informed consent was obtained from all participants involved in the study.

Human and Animal Rights Statement On behalf of all authors, the corresponding authors (Cole A. DeForest and Kelly R. Stevens) affirm that human and animal rights were upheld in the study.

Competing Interests The authors declare no competing interests.

References

We acknowledge that papers authored by women and scholars from historically excluded racial and ethnic groups are systematically under-cited. So that we are not further perpetuating this problem, we have made every attempt to reference relevant papers in a manner that is equitable in terms of gender and racial representation.

1. Mirshafiei M, Rashedi H, Yazdian F, Rahdar A, Baino F. Advancements in tissue and organ 3D bioprinting: current techniques, applications, and future perspectives. Mater Des. 2024;240: 112853. https://doi.org/10.1016/j.matdes.2024.112853.
2. Xu S, Ahmed S, Momin M, Hossain A, Zhou T. Unleashing the potential of 3D printing soft materials. Device. 2023;1(3): 100067. https://doi.org/10.1016/j.device.2023.100067.
3. Panja N, Maji S, Choudhuri S, Ali KA, Hossain CM. 3D bioprinting of human hollow organs. AAPS PharmSciTech. 2022;23(5):139. https://doi.org/10.1208/s12249-022-02279-9.
4. Murphy SV, Atala A. 3D bioprinting of tissues and organs. Nat Biotechnol. Aug.2014;32(8):773–85. https://doi.org/10.1038/nbt.2958.
5. Corbett DC, et al. Thermofluidic heat exchangers for actuation of transcription in artificial tissues. Sci Adv. 2020;6(40):eabb9062. https://doi.org/10.1126/sciadv.abb9062.
6. Kopyeva I, Brady RP, DeForest CA. Light-based fabrication and 4D customization of hydrogel biomaterials. Nat Rev Bioeng. 2024. https://doi.org/10.1038/s44222-024-00234-w.
7. Corbett DC, Olszewski E, Stevens K. A FRESH take on resolution in 3D bioprinting. Trends Biotechnol. 2019;37(11):1153–5. https://doi.org/10.1016/j.tibtech.2019.09.003.
8. Dhand AP, Davidson MD, Burdick JA. Lithography-based 3D printing of hydrogels. Nat Rev Bioeng. 2024;3:108–25. https://doi.org/10.1038/s44222-024-00251-9.
9. Grigoryan B, et al. Multivascular networks and functional intravascular topologies within biocompatible hydrogels. Science. 2019;364(6439):458–64. https://doi.org/10.1126/science.aav9750.
10. Zhang Z, Wang B, Hui D, Qiu J, Wang S. 3D bioprinting of soft materials-based regenerative vascular structures and tissues. Compos B Eng. 2017;123:279–91. https://doi.org/10.1016/j.compositesb.2017.05.011.
11. Richbourg NR, Rausch MK, Peppas NA. Cross-evaluation of stiffness measurement methods for hydrogels. Polymer. 2022;258: 125316. https://doi.org/10.1016/j.polymer.2022.125316.
12. Ma X, et al. Deterministically patterned biomimetic human iPSC-derived hepatic model via rapid 3D bioprinting. Proc Natl Acad Sci. 2016;113(8):2206–11. https://doi.org/10.1073/pnas.1524510113.
13. Guimarães CF, Gasperini L, Marques AP, Reis RL. The stiffness of living tissues and its implications for tissue engineering. Nat Rev Mater. 2020;5(5):351–70. https://doi.org/10.1038/s41578-019-0169-1.
14. Jandl K, Kwapiszewska G. Stiffness of the extracellular matrix: a regulator of prostaglandins in pulmonary fibrosis? Am J Respir Cell Mol Biol. 2020;63(6):721–2. https://doi.org/10.1165/rcmb.2020-0398ED.
15. Wang M, et al. Molecularly cleavable bioinks facilitate high-performance digital light processing-based bioprinting of functional volumetric soft tissues. Nat Commun. 2022;13(1):3317. https://doi.org/10.1038/s41467-022-31002-2.
16. Zhu M, et al. Gelatin methacryloyl and its hydrogels with an exceptional degree of controllability and batch-to-batch consistency. Sci Rep. 2019;3;9(1):6863. https://doi.org/10.1038/s41598-019-42186.
17. Yang M, et al. Multi-material digital light processing (DLP) bioprinting of heterogeneous hydrogel constructs with perfusable networks. Adv Funct Mater. 2024;2316456. https://doi.org/10.1002/adfm.202316456.
18. Schindelin J, et al. Fiji: an open-source platform for biological-image analysis. Nat Methods. 2012;9(7):676–82. https://doi.org/10.1038/nmeth.2019.
19. Sun Q, Hou Y, Chu Z, Wei Q. Soft overcomes the hard: flexible materials adapt to cell adhesion to promote cell mechanotransduction. Bioact Mater. 2022;10:397–404. https://doi.org/10.1016/j.bioactmat.2021.08.026.
20. Yi B, Xu Q, Liu W. An overview of substrate stiffness guided cellular response and its applications in tissue regeneration. Bioact Mater. 2022;15:82–102. https://doi.org/10.1016/j.bioactmat.2021.12.005.
21. Kopyeva I, et al. Stepwise stiffening/softening of and cell recovery from reversibly formulated hydrogel interpenetrating networks. Adv Mater. 2024;36(44):2404880. https://doi.org/10.1002/adma.202404880.
22. Taghizadeh RR, Cetrulo KJ, Cetrulo CL. Collagenase impacts the quantity and quality of native mesenchymal stem/stromal cells derived during processing of umbilical cord tissue. Cell Transplant. 2018;27(1):181–93. https://doi.org/10.1177/0963689717744787.
23. Bretherton RC, et al. User-controlled 4D biomaterial degradation with substrate-selective sortase transpeptidases for single-cell biology. Adv Mater. 2023; 2209904. https://doi.org/10.1002/adma.202209904.
24. Gharios R, Francis RM, DeForest CA. Chemical and biological engineering strategies to make and modify next-generation hydrogel biomaterials. Matter. 2023;6(12):4195–244. https://doi.org/10.1016/j.matt.2023.10.012.

Authors and Affiliations

Olivia P. Dotson[1,2] · Sherina Malkani[2,3,4] · Inkyung Kang[2,3] · Cole A. DeForest[1,2,3,5,6,7] · Kelly R. Stevens[1,2,3,8,9]

✉ Cole A. DeForest
profcole@uw.edu

✉ Kelly R. Stevens
ksteve@uw.edu

[1] Molecular Engineering and Sciences Institute, University of Washington, Seattle, WA 98195, USA

[2] Institute for Stem Cell and Regenerative Medicine, Seattle, WA 98195, USA

[3] Department of Bioengineering, University of Washington, Seattle, WA 98195, USA

[4] Department of Bioengineering, Rice University, Houston, TX 77005, USA

[5] Department of Chemical Engineering, University of Washington, Seattle, WA 98195, USA

[6] Department of Chemistry, University of Washington, Seattle, WA 98195, USA

[7] Institute for Protein Design, University of Washington, Seattle, WA 98195, USA

[8] Department of Laboratory Medicine & Pathology, University of Washington, Seattle, WA 98195, USA

[9] Brotman Baty Institute, Seattle, WA 98195, USA